Journal of Applied Polymer Science

Effect of the Host Polymer on the Nanomechanical and Morphological Properties of Templated Polymer Films

Sadik Antwi-Boampong,[1] Yuan Liu,[1] Asta Richter,[2] Joseph J. BelBruno[1]
[1]Department of Chemistry, Dartmouth College, Hanover, New Hampshire 03755
[2]Department of Engineering Science, Technical University of Applied Sciences, Wildau 15745, Germany
Correspondence to: J. J. BelBruno (E-mail: jjbchem@dartmouth.edu)

ABSTRACT: Atomic force microscopy and nanoindentation have been applied to the study of thin molecularly templated polymer films. The template was chosen to be the readily hydrogen-bonded cotinine molecule and three different polymer hosts, Elvamide® nylon, Nylon-6, and poly(4-vinylphenol) were compared. The host polymer was shown to affect the nature of the template-host interaction resulting in varying surface morphologies and differences in the nanohardness. These observations were shown to reflect differences in the underlying interaction chemistry, specifically, whether or not the polymer may be imprinted in the film production process. © 2013 Wiley Periodicals, Inc. J. Appl. Polym. Sci. 130: 877–883, 2013

KEYWORDS: properties and characterization; polyamides; morphology; microscopy; mechanical properties

Received 28 May 2012; accepted 6 March 2013; published online 8 April 2013
DOI: 10.1002/app.39250

INTRODUCTION

Molecular imprinting is a synthetic technique for the production of molecule specific receptors analogous to natural receptor binding sites without the cost or environmental sensitivity of the natural systems.[1–9] Molecularly imprinted polymers (MIPs) may be based on either chemical or physical interactions between the host polymer and the template (target) molecule, as well as on shape recognition. We have adapted a form of phase inversion imprinting to the production of thin, 300 nm to 5 μm, films via spin coating[10–12] typically using hydrogen bonding and shape interactions to form the network. However, not all attempts at MIP production are successful. Protocols that lead to MIP formation using a particular polymer host may fail to produce imprinted material with subsequent polymers. These unimprinted polymers, however, still reflect the presence of a potential templating molecule during production, resulting in more porous films than those deposited from a polymer solution that did not contain the added molecular component. Such films may still have a practical use. Thin (several hundred nm) films of porous polymers are useful in the creation of sensing elements.

We have previously reported[13–15] on the use of depth sensing nanoindentation[16–23] to study the nanomechanical properties of MIP films. In those studies, the nanohardness was dependent upon the functional state of the MIP. That is, whether the MIP is "as-produced," has had the template molecule removed or has had the template (or a related molecule) reinserted into the emptied MIP. That research focused on the production parameters such as spin coating speed, template concentration, post-production heating, etc. for a single networked solution. In the current report, we describe nanomechanical measurements and morphological studies for polymer films formed in the presence of cotinine, produced under analogous experimental conditions, based on three different polymer hosts and provide a rationale for the observed changes in the experimental observations with varying polymer. These changes reflect the presence in one instance, or absence in others, of imprinting in the films.

EXPERIMENTAL DETAILS

Production of Polymer Films

Films were produced by spin coating; a simple deposition technique that is sensitive to the composition and viscosity of the solution and the rotating speed of the plate.[24] Spin coating adds complexity to film formation since the exact physical and chemical processes cannot be adequately modeled. However, films produced using this technique were readily reproducible and with careful monitoring of the spin coating conditions, observed variation in the films with different chemical components may be attributed to chemical influences.

The sample solutions in this study were composed of 5 wt % of polymer dissolved in an appropriate solvent along with 5 wt % of cotinine. Control solutions only contain 5 wt % of polymer

in the same solvent, but were otherwise treated in the same manner as the sample solutions. Poly(4-vinylphenol), P4VP, and Nylon-6 were obtained from Polysciences, Inc. (MW = 22,000, T_g 150°C; MW = 18,000, T_m 215–250°C, respectively) and cotinine from Alfa-Aesar (98%). Elvamide® was graciously donated by DuPont. The solvents, for the 5% by weight solutions noted above, were dimethylformamide, 98% formic acid, and ethanol, dissolving P4VP, Nylon-6 and Elvamide®, respectively. Unpurged solutions were covered and stirred at room temperature for 24 h. The only exception is the Elvamide® solutions, which were stirred at 40°C to dissolve the polymer. Films were spin cast from these solutions onto 25 mm square glass microscope cover slips. Typically, the slides were prewashed on the spin coater with spectroscopic grade acetone and isopropyl alcohol prior to polymer solution deposition. The coating solution was dropped onto a stationary substrate and the spin coater was operated at 4000 rpm for 30 s with negligible ramp up time. The nylon-6 solution was extremely viscous and the viscosity decreased for the Elvamide and P4VP polymer solutions. The rotation spread the solution evenly over the surface and also caused the solvent to evaporate leaving a thin film of solid material on the substrate. Film thickness was measured by a Veeco Dektak 150 Surface Profilometer. Cast films were quite stable and may be stored for an indefinite time.

If desired, the template molecule may be removed from the film by immersion in deionized water. Removal was confirmed by FTIR measurements. Template reinsertion, typically to a maximum of ~ 50% of the initial concentration, was accomplished by immersion of the sample film in a 5 wt % solution of the template molecule in deionized water for 2.5 h, again confirmed by infrared spectroscopy.

For comparison, control films of pure polymers were treated under the same chemical extraction conditions.

Nanoindentation Measurements

All nanoindentation experiments were performed using the electrostatic transducer of the Hysitron Triboscope in the UBI 1[25] with a Berkovich diamond tip. The data consisted of a load - displacement curve; for soft polymer samples, the stiffness of the internal springs holding the indenter must be subtracted from the applied load in order to obtain the sample stiffness. Hardness, H, was calculated in the standard format[17]; applied load, F, divided by the area, A_c, of the indenter tip at the contact depth, h_c. The calibration of the tip to determine the depth dependent area function $A_c(h_c)$ was obtained with the standard curve-fitting method using fused quartz with its known reduced modulus as the reference material. Thermal drift was measured and the effect was compensated in the resulting data. Hardness measurements of a thin layer of soft material on top of a harder glass substrate represent a complex system, since the hardness value contains contributions from the hard substrate unless the penetration depth is less than 10 % of the layer thickness (Bückle rule). Our measurements have been performed to a depth of 350 nm with an applied maximum load of up to 500 μN. Due to film softness, these penetration values often exceed the 10 % rule, thus corrections have been applied according to[26]:

$$\frac{H}{H_s} = 1 + \frac{H_f}{H_s} exp\left[\left(\frac{H_f}{H_s}\right)\left(\frac{h_c}{t_f}\right)/\left(\frac{\sigma_f}{\sigma_s}\right)\left(\frac{E_f}{E_s}\right)^{\frac{1}{2}}\right] \quad (1)$$

where, H_s and H_f are the hardness values, E_s and E_f are the Young's moduli and σ_s and σ_f are the yield strengths for the glass substrate and the soft polymer film, respectively. H is the measured hardness of the composite at the contact depth h_c and t_f is the film thickness. The hardness of the glass substrate was substantially greater than any measured values in our study with H_{glass} = 6 GPa and the glass indentation modulus was 70 GPa. The yield strength of the glass was approximated by H_{glass}/3. The indentation modulus and yield strength reported[27] for nylon were E_f = 3 GPa and σ_f = 45 MPa.

If loading and unloading are repeatedly performed, a multi-cycling experiment, at the same location on the sample surface, depth dependent mechanical properties are obtained.[15,18,23] As described in previous reports,[18] multi-cycling means, after loading to a maximum load, F_{max}, the sample is partially unloaded to a minimum load, F_{min} = 0.1 F_{max}, required to prevent the tip from losing contact with the sample. The sample is then reloaded to an increased maximum load (F_{max} + ΔF) and the cycle is repeated at the same location of the tip. Multi-cycling delivers a data set that includes the entire material response. Some samples were treated in this manner to probe the homogeneity of the film. Average values are obtained from several measurements at different locations on the same sample set.

AFM Characterization

Scanning force microscopy was applied to study the morphology of grain and pore formation in the polymer films, as well as surface roughness. For the data reported here, a Pacific Nanotechnology AFM Nano-I Microscope was used in close contact mode. The experiments used silicon tips with a resonant frequency of 300 kHz and a spring constant of 40 N m^{-1}. The surface topography of the films was characterized by average roughness measurements, R_a, defined as the average deviation of the profile from a mean line or the average distance from the profile to the mean line over the length of the assessment.

FTIR Characterization

FTIR spectra were recorded in the energy range from 4000 to 800 cm^{-1} using attenuated total reflection at 1 cm^{-1} resolution. The results were used as qualitative indications of the presence or absence of the cotinine template in the film. The presence of cotinine could be established by observation of characteristic absorption bands in the carbonyl and fingerprint regions of the spectrum.

RESULTS AND DISCUSSION

The presence and/or removal of cotinine in the films were confirmed by infrared spectroscopy. Examples of the spectra obtained in the study are shown in Figure 1 for nylon-6. The presence of cotinine in the sample films was indicated by the additional carbonyl peak at 1668 cm^{-1}, shown in the light green spectrum as compared to the absence of this feature in the red, control spectrum. When the cotinine was extracted, the blue spectrum was obtained, which was identical to the control spectrum. Reinsertion of cotinine from a 5% solution in water or

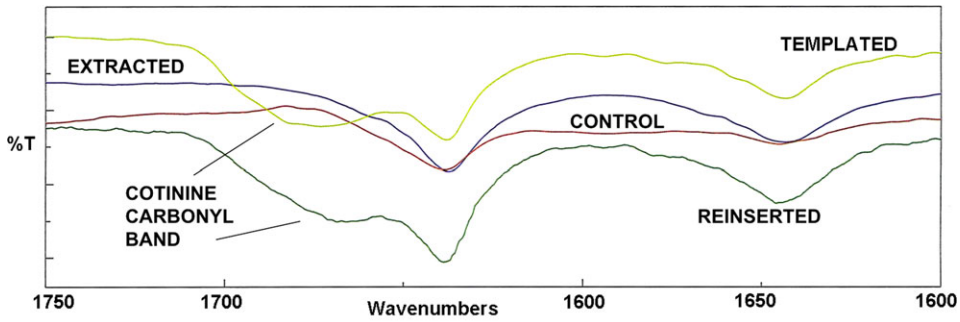

Figure 1. Attenuated total reflection infrared spectra of nylon-6 films: control (red), cotinine templated (light green), extracted templated films (blue) and reinserted cotinine films (dark green). [Color figure can be viewed in the online issue, which is available at wileyonlinelibrary.com.]

toluene restores the presence of the cotinine carbonyl band, as shown in Figure 1 (dark green spectrum). Identical treatment of a control film, including attempts at introducing adsorption of cotinine, does not yield evidence of cotinine readsorption in the infrared spectrum, providing assurance that the reintroduction of the template was due to the presence of cotinine in the original film.

In general, we found that sample films were more porous than the corresponding control films. Figure 2 presents AFM images for nylon control-sample pairs where the host polymer is either nylon-6 or Elvamide® nylon. The 5% nylon-6 control film image consisted of characteristically large crystalline grains amid some amorphous regions of polymer, in confirmation of previous results.[14] We demonstrated that the nylon-6 control film morphology was determined by parameters such as polymer concentration, spin coating conditions and temperature. The crystalline grains in this film average approximately 3–4 μm in diameter and were generated by nucleation as the spin coating solution dried from the air-liquid interface down to the substrate during solvent evaporation. Evaporation resulted in local nylon concentration increases, producing the granules. The film was clearly non-porous. The Elvamide® control film shown in Figure 2(c) was significantly less crystalline, as might be expected by its solubility in organic solvents. While one may discern very small grains in the film image, it was primarily an amorphous and, definitively not, a porous material. Disorder

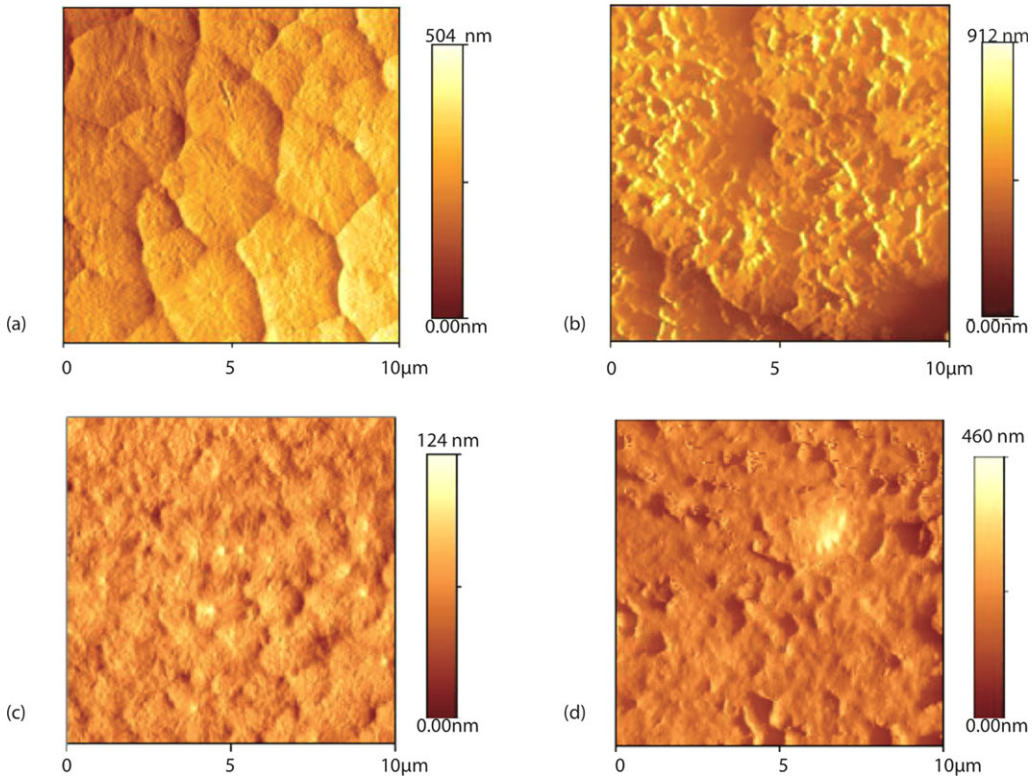

Figure 2. AFM images (10 μm square) of nylon-6 (a) control and (b) templated polymer films produced from 5% solutions of polymer and template and spin coated at 4000 rpm. Elvamide® control (c) and (d) templated films produced under the same conditions. [Color figure can be viewed in the online issue, which is available at wileyonlinelibrary.com.]

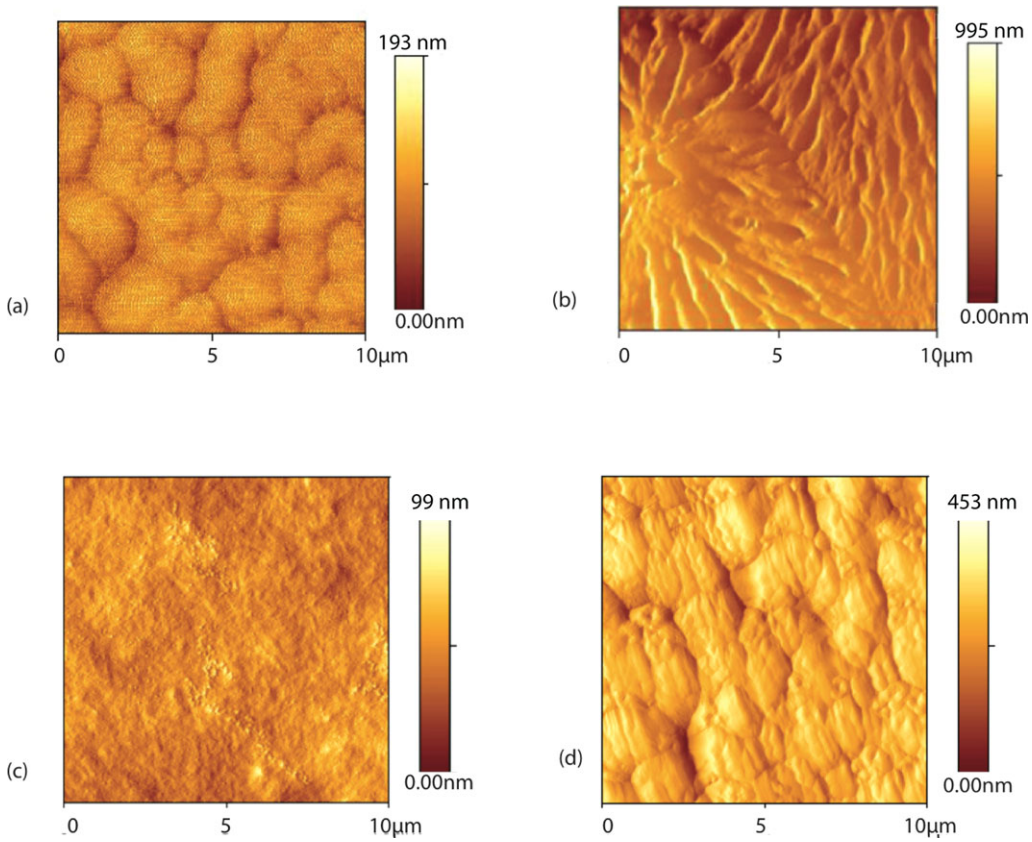

Figure 3. AFM images (10μm square) of extracted nylon-6 (a) control and (b) extracted templated polymer films produced from 5% solutions of polymer and template and spin coated at 4000 rpm. Extracted Elvamide® control (c) and (d) extracted templated films produced under the same conditions. Control films, even though not containing cotinine template, were subjected to the same extraction chemistry applied to the templated films. [Color figure can be viewed in the online issue, which is available at wileyonlinelibrary.com.]

among the polymer chains in this host precluded nucleation and large grain formation during spin coating and solvent evaporation, leading to the cited amorphous state of the film. While the extent of crystallinity varies between the two types of nylon, the measurements undertaken in this study are of nanomechanical properties, not crystallinity, although the latter property may be reflected in our measurements. We compare results for the sample films with a control for the same polymer, therefore, native crystallinity does not play a role in such measurements.

The sample films containing the template molecule, referred to as the "as produced" films, exhibited a much different morphology in comparison to the control films, as shown in Figures 2 and 3. Both sample films exhibited substantial porosity, clearly brought about by the presence of the cotinine molecule during film growth, since that was the only distinguishing difference in the sample material as compared with the control films. The height scale for both sample films increased dramatically in comparison to the respective control films.

The morphologies of the sample films changed when the template molecule was extracted in water, although the height scales of the films before and after extraction were similar. The porous morphology of both sample films was replaced by a more coherent appearance. Considering first the case of nylon-6, the sample film morphology became network-like, but most importantly, the free volume available within the "as produced" film, Figure 2(b), was no longer present and one would predict that the nanomechanical properties would become stiffer after extraction of the template from the sample film. Identical treatment of the control films did not afford the same drastic change in morphology. The dimensions of the large grains in the nylon-6 control film were reduced, perhaps due to slight swelling caused by water used for template extraction, however, the basic morphology of this film was unchanged.

The Elvamide® films followed the same general trend after extraction in water: the control film exhibited less height variation after treatment, it becomes smoother, and the sample film lost porosity after extraction of the template molecule. These images are also contained in Figure 3.

Thickness measurements indicated that the film dimension depended upon the state of the sample film. Control films were considerably thinner (~500 nm and 500–800 nm, for nylon-6 and Elvamide®, respectively) than sample films in the as produced (800 nm and up to 2600 nm) or extracted (1600 nm and 2000 nm) functional states. The presence of the template molecule led to thicker nylon films, even though an identical quantity of solution was deposited on the substrate. The cotinine did not significantly interact chemically with the host polymer. This is confirmed by the nanohardness measurements that will be

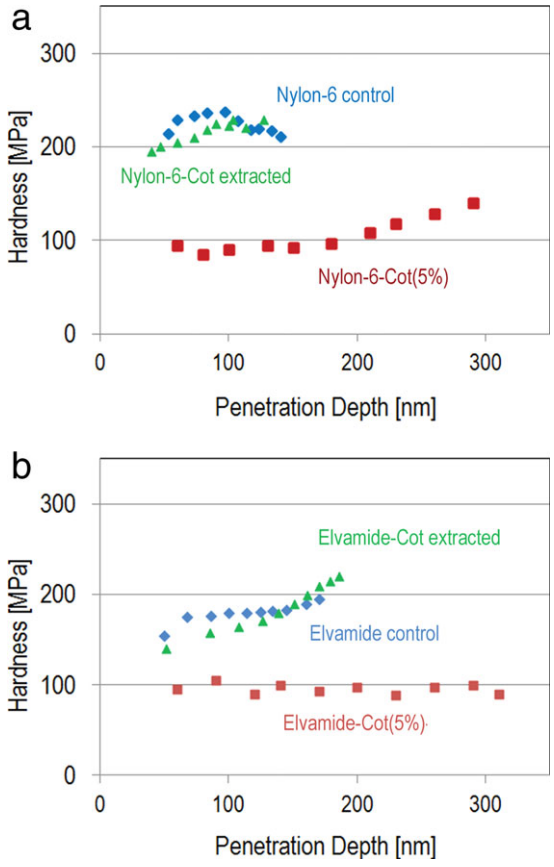

Figure 4. Depth dependent hardness values for (a) Nylon-6 and (b) Elvamide® based templated films: control, as produced Cot(5%) templated and extracted templated films. [Color figure can be viewed in the online issue, which is available at wileyonlinelibrary.com.]

described below. The extraction procedure further increased the film thickness due to swelling by the extraction solvent, but provided a means for increased polymer-polymer interactions and increased hardness. The average surface roughness measurements confirmed the qualitative conclusions drawn from the height scales of the AFM images. In general, the nylon-6 films were rougher than the Elvamide® films. Over a 30μm square sample, the nylon-6 and Elvamide® control films had R_a values of 45.7 nm and 15.2 nm, respectively. The sample films, however, had roughness values of 70.7 nm and 22.6 nm, respectively. The presence of the cotinine during film production increased the roughness.

The measured nanohardness values at 200 μN of applied force are shown in Figure 4.

The comparison of the depth dependent hardness values for different functional sample states is difficult, since for thin films the influence of the glass substrate is visible. Thus, the values were corrected with formula (1), but original data were retained, when possible. The hardness of the Elvamide® control film shows a dominant plateau before the hardness further increases at a penetration depth of 160 nm indicating the presence of the glass substrate, Figure 4(b). The nylon-6 control film had a thickness of $\sim$ 500 nm and the correction, eq. (1), was applied to correct the hardness values. For large penetration depths, eq. (1) reduces the effective hardness severely, so that there is a slight hardness decrease visible in Figure 4(a). The control samples for the two nylon polymers provided similar nanohardness results, 180 MPa for Elvamide® and 224 MPa for nylon-6 (Table I). The nanohardness results for 5 wt % cotinine containing films exhibited the same trend of extremely low values. Since the as-produced films are thicker, a correction of hardness data was not necessary. The corresponding curves in Figure 4 clearly show a plateau over a large region of the penetration depth. At about 200 nm penetration depth, the hardness for nylon-6 starts to increase due to the influence of the harder glass substrate. In the case of the cotinine loaded Elvamide® film, the nanohardness was reduced to 96 MPa, while the nylon-6 cotinine loaded film had a nanohardness of 105 MPa. If the cotinine content is further increased to 10 wt %, the hardness value for Elvamide® film drops drastically to 47 MPa. Extracted nylon cotinine templated films exhibited a nanohardness close to the values shown by the control samples: for Elvamide®, 185 MPa and for nylon-6-cotinine extracted, 216 MPa (Table I). The extracted Elvamide® cotinine film [Figure 4(b)] shows a slight increase of the hardness with increasing depth before the hardness steeply increases at 165 nm indicating the influence of the glass substrate. The steep incline could not be corrected with eq. (1) due to the measured film thickness of 1360 nm. The large standard deviation for extracted Elvamide-cotinine films of 14.6% may indicate a hardness gradient over the polymer film.[28] The inhomogeneities over the film cross section may be caused by chemical interactions during extraction of the template molecule. The extracted nylon-6 cotinine films exhibited such a hardness gradient in the original data set. Up to a penetration depth of 80 nm, the hardness values were between 195 and 210 MPa. Then a steep increase was observed and hardness values were corrected by formula (1) with a film thickness of 800 nm. The result is displayed in Figure 4(a).

Table I. Comparison of Average Hardness Values H_{av} and Their Standard Deviation of Functional States with Control, Cot(5%) and Extracted for Elvamide, Nylon-6, and PVP-Based Films

	Elvamide control	Elvamide-Cot(5%)	Elvamide-Cot extracted	Nylon-6 control	Nylon-6-Cot(5%)	Nylon-6 extracted	PVP control	PVP-Cot-MIP	PVP extracted
H_{av} [MPa]	180	96	185	224	105	216	380	580	320
Standard deviation [MPa]	10	5	27	10	7	12	14	35	21
%	5.6	5.2	14.6	4.5	6.8	5.6	3.7	6.0	6.5

This trend was in stark contrast to the results obtained for P4VP and provided in Table I for comparison. Templated P4VP films were confirmed to be imprinted by binding studies.[14] For this polymer host, the control film had a measured hardness of 380 MPa, MIP films were harder, 595 MPa and extracted films were softer, but closer to the hardness of the control film, 300 MPa.[13] These results implied that significant chemical interactions between template and polymer host were operative in the P4VP films.

Spin coating is a complex process, typically divided in to four distinct phases. For our purposes, we may consider AFM-visualized morphology a result of the fourth phase. In that realm, evaporation of the solvent in the upper or outer layer of the film enriches that portion in both template and polymer, relative to lower regions. Attractive forces between the chemical components and the substrate also play a role in the developing morphology. The AFM images pointed to nylon sample films that, rather than contain the pores produced in a spin coated film by a porogen when the film solidifies during spinning as is commonly observed in MIP films hosted in P4VP, were uniformly porous. Given the semicrystalline nature of the nylon-6 control film, the porosity of both nylon sample films must be attributed to the presence of the cotinine template molecule. Cotinine molecular imprinting using poly(4-vinylphenol) as the host polymer creates a situation in which the template-containing MIP has a nanohardness that is greater (580 MPa) than the unimprinted control film (380 MPa), while the extracted MIP is significantly softer (300 MPa) than the control. The current nylon observations were a stark contrast to the P4VP study: for the nylons, the template-containing film was softer than the control and the hardness of the template-extracted film approximated that of the control film. The P4VP MIP results were attributed to a combination of the influence of the spin coating conditions and hydrogen bonding of the template molecule with the polymer host. The latter aspect of the P4VP MIP morphology was confirmed by shrinkage within the film and the observation of a further increase in the nanohardness when the template molecule was reinserted into an extracted P4VP hosted MIP. The P4VP-cotinine studies produced an imprinted film that contained numerous large pores at somewhat regular intervals. Since spin coating conditions in the current research were identical to those used in the P4VP study, the unique behavior of our nylon films must attributed to the absence of the MIP type of interaction between the polymer host and the cotinine molecule.

Elvamide® is a mixture of nylon-6, nylon-6,6 and nylon-6,10. The solubility of the material in hot alcohol is a result of the disorder brought about by the mixture of nylon polymers, leading to the absence of both homogeneous hydrogen bonding among the chains of the individual components and heterogeneous hydrogen bonding among unlike nylon chains. The fact that the polymer host and the template were present in equal concentrations increased this heterogeneity and further decreased the probability of hydrogen bonding among any of the components. The increased disorder and absence of any hydrogen bonding that might be present in the control film produced a templated film having an extremely smaller nanohardness. The template molecular binding site may be described simply as a cavity formed by the Elvamide® polymer solidifying around the cotinine. We speculate that there was little significant chemical interaction between the polymer host and the template and no evidence of hydrogen-bonded complexes was found in the infrared spectra.

The nylon-6 cotinine films exhibited morphological and nanomechanical properties similar to those just recounted for Elvamide®. The nylon-6 control films and the extracted nylon-6 cotinine films had similar nanomechanical properties and the films containing the template were significantly softer than those of the control or extracted film states. The starting material, nylon-6 polymer is homogeneous, therefore, the nanomechanical properties, as was true for the morphological observations, must result from the heterogeneity of the film solution that was composed of equal parts polymer and template molecule.

SUMMARY

We have demonstrated that an extremely porous polymer film may be produced using an alcohol soluble nylon (Elvamide®) host polymer. The same effect may be generated using the solvent resistant nylon-6 polymer host, if the concentration of the templating molecule approximates that of the host polymer. The porosity of the templated films leads to material with very low nanohardness. As a result, no hydrogen bonds are formed between the cotinine and these host polymers and the effect of imprinting is considerably reduced. This situation is in strong contrast to the treatment of P4VP with cotinine, where recognition places are produced and a proper molecular imprinting was achieved.

An important aspect of the research described here is the generalization that a disordered system may be used to create an extremely porous material. From the nanomechanical and AFM investigations, it is suggested that disorder

1. precludes the formation of polymer–polymer and polymer–template hydrogen bonds,
2. creates a film with the template molecules scattered throughout the host polymer,
3. enhances gliding separation of the polymer strands and
4. lowers the forces between polymer molecules.

The technique is useful not only for the creation of films with pseudo-selective properties, but also for the production of a class of porous polymer materials that may find other, nonextractive applications.

ACKNOWLEDGMENTS

J.J.B. acknowledges the financial support from the American Academy of Pediatrics through the Richmond Center for Excellence funded by the Flight Attendants Medical Research Institute. A.R. acknowledges the Harris Distinguished German Professorship from Dartmouth College, which supported a research visit during which this work was completed.

REFERENCES

1. Marty, J. D.; Mauzac, M. *Adv. Polym. Sci.* **2005**, *172*, 1.
2. Dufaud, V.; Bonneviot, L. In Nanomaterials and Nanochemistry, Brechignac, C.; Houdy, P., Lahmani, M., eds. Springer: Berlin, **2008**, 597.
3. Kempe, H.; Kempe, M. In The Power of Functional Resins in Organic Synthesis, Tulia-Puche, J.; Fibericio, F., eds. Wiley: Berlin, **2008**.
4. Poma, A.; Turner, A. P. F.; Piletsky, S. A. *Trends Biotechnol.* **2010**, *28*, 629.
5. BelBruno, J. J. *Micro Nanosystems* **2009**, *1*, 163.
6. Yanga, K.; Maa, J.; Hzhoub, H.; Lia, B.; Yua, B.; Zhaoa, C. *Desalination* **2009**, *245*, 232.
7. Faizala, C. K. M.; Kikuchic, Y.; Kobayashi, T. *J. Membr. Sci.* **2009**, *334*, 110.
8. Dima, S. O.; Sabru, A.; Dobre, T.; Bradu, C.; Antohe, N.; Radu, A.; Nicolescui, T.; Lungu, A. *Mater. Plastice* **2009**, *46*, 372.
9. Chen, R. R.; Qin, L.; Jia, M.; He, X. W.; Li, Y. *J. Membr. Sci.* **2010**, *363*, 212.
10. Shneskoff, N.; Crabb, K.; BelBruno, J. J. *J. Appl. Polym. Sci.* **2002**, *86*, 3611.
11. Richter, A.; Gibson, U. J.; Nowicki, M.; BelBruno, J. J. *J. Appl. Polym. Sci.* **2006**, *101*, 2919.
12. Campbell, S. E.; Collins, M.; Lei, X.; BelBruno, J. J. *Surf. Interface Anal.* **2009**, *41*, 347.
13. Richter, A.; BelBruno, J. J. *J. Appl. Polym. Sci.* **2012**, *124*, 2798.
14. BelBruno, J. J.; Richter, A.; Campbell, S. E.; Gibson, U. J. *Polymer* **2007**, *48*, 1679.
15. Richter, A.; Gruner, M.; BelBruno, J. J.; Gibson, U. J.; Nowicki, M. *Coll. Surf. A* **2006**, *284/285*, 401.
16. Fischer-Cripps, A. C. Nanoindentation; Springer: New York, **2002**.
17. Olivier, W. C.; Pharr, G. M. *J. Mater. Res.* **1992**, *7*, 1562.
18. Wolf, B.; Richter, A. *New J. Phys.* **2003**, *5*, 15.
19. Ward, I.M.; Hadley, D. W. An Introduction to the Mechanical Properties of Solid Polymers; Wiley: Chichester, **1993**.
20. Nowicki, M.; Richter, A.; Wolf, B.; Kaczmarek, H. *Polymer* **2003**, *44*, 6599.
21. Du, B.; J. Liu, J.; Q. Zhang, Q.; T. He, T. *Polymer* **2000**, *42*, 5901.
22. Tsui, O. K.; Wang, X. P.; Ho, J. Y. L.; Nag, T. K.; Xiao, X., *Macromolecules* **2000**, *33*, 4198.
23. Richter, A.; Smith, R. *Encyclopedia Nanosci. Nanotechnol.* **2011**, *17*, 375.
24. Bronside, D. E.; Macosko, C. W.; Scriven, L. E. *J. Imaging Technol.* **1987**, *13*, 122.
25. Hysitron User Handbook: Feedback Control Manual. 10025 Valley View Road, Minneapolis, MN 55344, USA; Hysitron, Inc.
26. Bhushan, B.; Xiaodong, L. *Int. Mater. Rev.* **2003**, *48*, 125.
27. Available at: http://www.engineeringtoolbox.com/young-modulus-d_417.html; The Engineering Toolbox.
28. Almaral-Sanchez, J. L.; Lopez-Gomez, M.; Ramirez-Bon, R.; Munoz-Saldana, J. *J. Mater. Online* **2006**, *2*, 0191.